Vacancy-enhanced ferromagnetism in Fe-doped rutile TiO_2

Jun Chen,[1,2] Paul Rulis,[1] Lizhi Ouyang,[3] S. Satpathy,[4] and W. Y. Ching[1,*]
[1]*Department of Physics, University of Missouri-Kansas City, Kansas City, Missouri 64110, USA*
[2]*Institute of Applied Physics and Computational Mathematics, Beijing, China, 100088*
[3]*Department of Physics and Mathematics, Tennessee State University, Nashville, Tennessee 37221, USA*
[4]*Department of Physics, University of Missouri, Columbia, Missouri 65211, USA*
(Received 30 September 2006; published 8 December 2006)

Based on a series of supercell density functional calculations of Fe-doped TiO_2 both with and without O vacancy (V_O), we show that V_O plays an important role in determining the magnetic properties of the dilute magnetic semiconductors (DMS). Without V_O, two Fe atoms in rutile lattice are ferromagnetically coupled except at a separation distance of 3.57 Å, where they are antiferromagnetically coupled. The V_O introduces two electrons into the conduction bands of rutile, which are either captured by the Fe dopants or form a shallow impurity state. The ferromagnetic (FM) coupling J between two Fe atoms is enhanced, through the enhancement of the FM double exchange if V_O is sufficiently close.

DOI: 10.1103/PhysRevB.74.235207 PACS number(s): 75.50.Pp, 61.72.Ji, 75.10.Lp, 75.30.Hx

I. INTRODUCTION

Recent studies on dilute magnetic semiconductors (DMS) for room temperature spintronics applications concentrate mostly on Mn-doped GaAs (Refs. 1–3) and GaN compounds.[4,5] Co doped TiO_2 was also reported to be a promising magnetic oxide semiconductor (MOS) with n type of carriers.[6,7] However, the reported Curie temperature T_c is quite low which limits its practical applications. Furthermore, controversies regarding the nature of the samples arise and much of the claim cannot be validated.[8–11] More recently, it was reported that doping Fe in reduced rutile has p-type carriers and a higher T_c [Ref. 12]. The reported magnetic moment per Fe (M_s) is as high as 2.4 μ_B. The possibility of room temperature ferromagnetic semiconductors with a high T_c is very exciting. There have been several reports on Fe doping in TiO_2 with conflicting results and interpretations[13–19] which could be the source of much of the discrepancy. These different observations arise from different samples prepared in different laboratories. The atomic-scale structure of Fe-doped TiO_2 has not been precisely characterized and there are lingering doubts as to the validity of the data and the origin of the observed ferromagnetism (FM). Most likely, the presence of O vacancies (V_O) in these materials play an important role but this has not been thoroughly investigated.

To understand the role of the vacancies in determining the magnetic properties of the oxide-based DMS, we study the Fe-doped rutile TiO_2 with and without V_O using density functional theory (DFT). We find that vacancies enhance the FM in two distinctly different ways, either through the formation of a shallow impurity state of a nearest-neighbor Fe -V_O complex or through the capture of the vacancy electrons by the Fe atoms and the subsequent enhancement of the FM double exchange. In the next section, we briefly outline our method of calculation. The results of the supercell calculations on Fe-doped TiO_2 without and with V_O are presented and discussed in Sec. 3. The last section is for conclusions, emphasizing the importance of O vacancy in dilute magnetic oxide semiconductors.

II. METHOD OF CALCULATION

The rutile TiO_2 crystallizes in a tetragonal cell (a =4.594 Å, c=2.959 Å, space group $P4_2/mnm$). In this study, we used a $2\times2\times4$ supercell (32 Ti and 64 O atoms) and replace Ti atoms by one, two or three Fe atoms corresponding to concentration ratios of x=1/32, 1/16, and 3/32 in $(Fe_xTi_{1-x})O_2$ which are close to the experimentally reported values[12] of x=0.02, 0.06, and 0.08. We then considered the cases of single V_O, 1 Fe and 1 V_O, 2Fe and 1 V_O, and 1 Fe and 2 V_O. For a 96-atom supercell, the maximum interatomic separations for Ti-Ti, Ti-O, and O-O are restricted to 7.49 Å, 6.88 Å, and 7.48 Å, respectively because of the periodic boundary condition. In each case, a large number of defect configurations were identified for *ab initio* study. For each model, the structure was fully relaxed using DFT as implemented in the Vienna *ab initio* Simulation Package (VASP) in the spin-polarized mode.[20,21] We used the PWA-GGA potential for the exchange and correlation and a high energy cutoff of 600 eV. Eight k points were used in the irreducible Brillouin zone of the supercell. The total energy (TE) attained an accuracy of at least 0.001 eV and the residual force converged to about 0.01 eV/Å. For perfect TiO_2, VASP results show a slight expansion of the lattice (1% for a, 0.7% for c). The calculated vacancy formation energy for V_O is 2.71 eV. This accuracy is fairly typical of calculations based on DFT. Substitution of a Ti by an Fe reduces the supercell size slightly and the Fe-O bonds (1.904 Å, 1.908 Å) are shorter than the original rutile Ti-O bonds (1.949 Å and 1.980 Å). They are comparable to the Fe-O bonds in Fe_3O_4 (1.862 Å and 1.936 Å). The energy of substitution for a single Fe is 4.18 eV. The calculated Fe moment (M_S) and that of the whole cell are 1.67 μ_B and 1.72 μ_B, respectively since the neighboring O ions are found to be slightly polarized in the same direction.

III. RESULTS AND DISCUSSION

Figures 1(a) and 1(b) shows the density of states (DOS) of TiO_2 with 1 V_O and 1 Fe, respectively. The one electron DOS

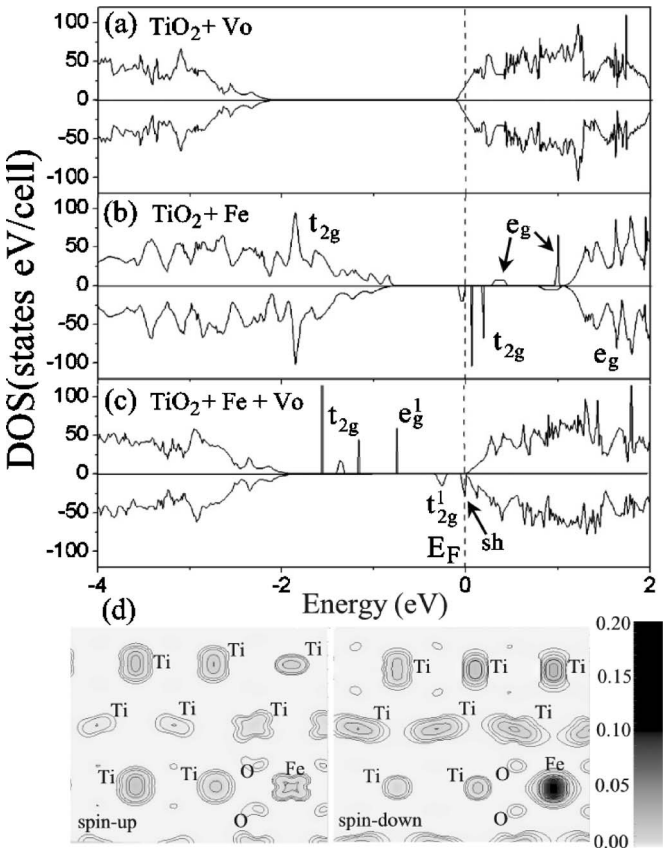

FIG. 1. Total DOS of supercell models: (a) TiO_2+V_O; (b) TiO_2+Fe; (c) TiO_2+V_O+Fe at the NN separation of 1.94 Å; (d) charge density (in unit of electron/cell volume) of the shallow state in (c) near E_F.

of TiO_2 (not shown) is hardly changed upon the introduction of the V_O, except that the vacancy introduces two additional electrons into the conduction band (CB) more-or-less in a rigid-band fashion. These electrons are populated at the bottom of the CB made up of the Ti-3*d* orbitals and they are delocalized over the entire crystal. For the case of an Fe atom substituted at the Ti site, the occupied electronic configuration of Fe is $d^4(t_{2g}^3\uparrow, t_{2g}^1\downarrow)$, where we have adopted the symmetry notations of the local octahedral crystal field, which splits the Fe(*d*) states into the triply-degenerate t_{2g} state and the doubly-degenerate e_g state, the latter occurring at the higher energy. The $t_{2g}^3\uparrow$ states merge with the top portion of the valence band (VB) of O-2*p* character. Right below the Fermi level (E_F) is the occupied $t_{2g}^1\downarrow$ state out of the manifold of the three t_{2g} states. These symmetry states are split further by the crystal field as can be seen from Fig. 1.

The electronic structure of Fe is drastically changed in the presence of V_O. Of particular interest is the emergence of a shallow impurity state (labeled *sh*) at the bottom of the CB in the minority spin channel as indicated in Fig. 1(c), if the Fe and V_O are the nearest neighbor (NN). If the vacancy is further away, then the two electrons are merely donated to the Fe atom which either forms in the $(t_{2g}^3\uparrow, t_{2g}^3\downarrow)$ state or in the $(t_{2g}^3\uparrow e_g^1\uparrow, t_{2g}^2\downarrow)$ state (see Fig. 3 below). The shallow sh is quite delocalized as illustrated in Fig. 1(d), spreading out to several Ti sites.

We next consider the case of 2 Fe with no V_O. Figure 2 shows the TE and M_S as a function of Fe-Fe separation $d_{Fe\text{-}Fe}$. A striking feature is that M_s is fairly constant at about 1.87 μ_B except at $d_{Fe\text{-}Fe}$=3.57 Å where the two Fe moments are antiferromagnetically (AF) coupled and the TE is the lowest. The magnetic interactions between the Fe atoms are the result of the competition between the AF superexchange

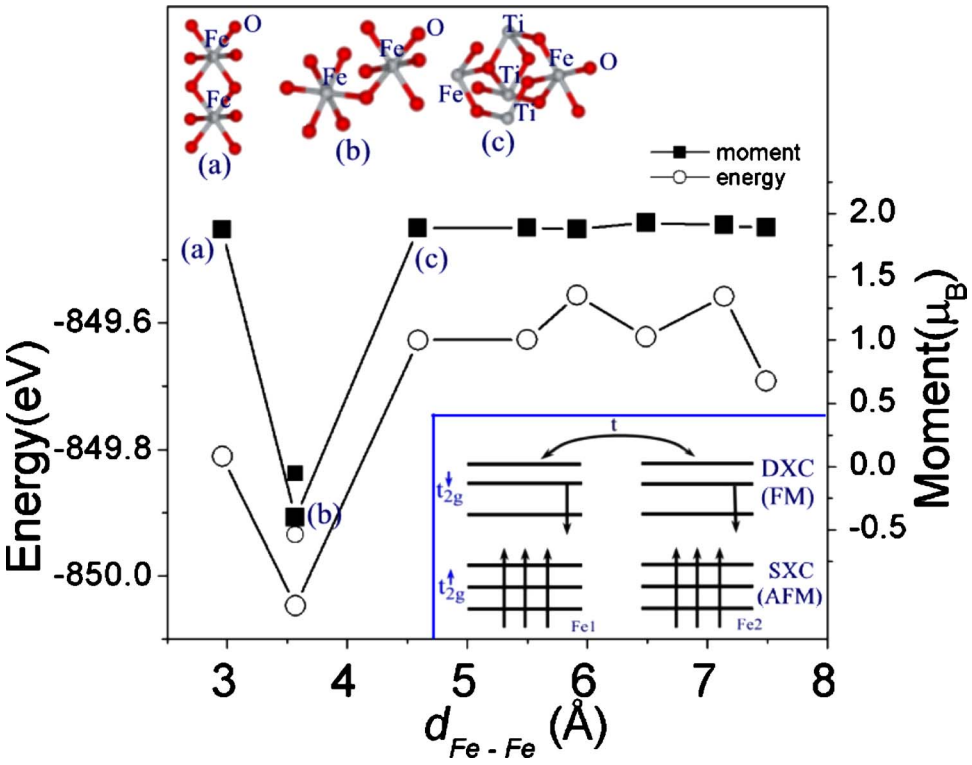

FIG. 2. (Color online) Total energy (open circle) and magnetic moment per Fe (solid square) in the 2 Fe model as a function of $d_{Fe\text{-}Fe}$. The connecting lines are just guides to the eye. The insets show the local geometry of the first three data points (upper left) and the illustration (lower right) of the possible DXC and SXC models that lead to the FM and AF ground states.

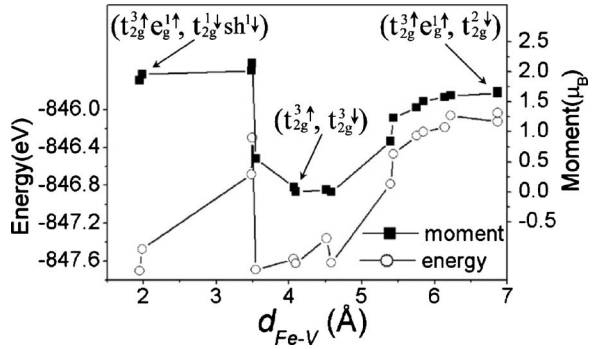

FIG. 3. Total energy (open circle) and magnetic moment per Fe (solid square) in the Fe+V_O model as a function of $d_{Fe\text{-}V}$. The electronic structures of the Fe from the DOS study for three different $d_{Fe\text{-}V}$ are as indicated.

(SXC) and the FM double exchange (DXC),[22,23] which are determined by local atomic arrangements and local orbital ordering, which control the magnitude of the two competing interactions.[24] The inset of Fig. 2 shows the local configurations of the first three data points (a), (b), and (c). For (a), the two Fe ions are linked by two Fe-O-Fe paths ($d_{Fe\text{-}Fe}$ =2.95 Å). For (b), the two Fe are linked by only one Fe-O-Fe path with $d_{Fe\text{-}Fe}$=3.57 Å. For (c), the two Fe are linked with three separate Fe-O-Ti-O-Fe chains and a larger separation ($d_{Fe\text{-}Fe}$.=4.59 Å). The DOS results show the electronic configuration of Fe to be $d^4(t_{2g}^3\uparrow, t_{2g}^1\downarrow)$, just like the case for the isolated Fe impurity shown in Fig. 1(b). Magnetism is determined by a competition between the SXC interaction between the filled $t_{2g}\uparrow$ electrons, which is AF and the DXC interaction between the $t_{2g}\downarrow$ electrons, which is FM. The latter depends on the electron hopping between the neighboring Fe atoms and therefore depends on the orbital orientations of the two $t_{2g}\downarrow$ electrons of the neighboring atoms. If the orbital orientation is such that the hopping is small, the AF-SXC dominates as in case (b), while if the hopping is large, the FM-DXC overwhelms the AF-SEX, producing a net FM interaction as in case (a). The inset in the lower right part of Fig. 2 illustrates this competition.

In reduced samples of Fe-doped TiO_2, O vacancies are present. Experimentally, precise estimation of the location and concentration of V_O is very difficult. To understand the role of V_O, computational modeling is *sine qua non*. However, the magnetic behavior is far more complicated since Fe-V_O and V_O-V_O separations (denoted by $d_{Fe\text{-}V}$ and $d_{V\text{-}V}$, respectively) are additional parameters that affect the overall magnetic interaction. Figure 3 shows the TE and M_S for 16 models of 1 Fe and 1 V_O as a function of $d_{Fe\text{-}V}$. The TE data suggest that the V_O prefers to be at the NN site of Fe ($d_{Fe\text{-}V}$=1.94 Å or 1.98 Å) or at intermediate $d_{Fe\text{-}V}$ of 3.5 Å to 4.6 Å. At $d_{Fe\text{-}V}>5.4$ Å, or for $d_{Fe\text{-}V}$ slightly less than 3.5 Å, the model is energetically less favorable.

The electronic structure of Fe in presence of V_O shows two distinct characteristics. As discussed earlier, the vacancy potential is not strong enough to produce a bound state for the electrons; rather they occupy the CB in a rigid-band fashion. We find that if the V_O is next to Fe ($d_{Fe\text{-}V}$=1.94 Å), then we have altogether six electrons, five of which are in the

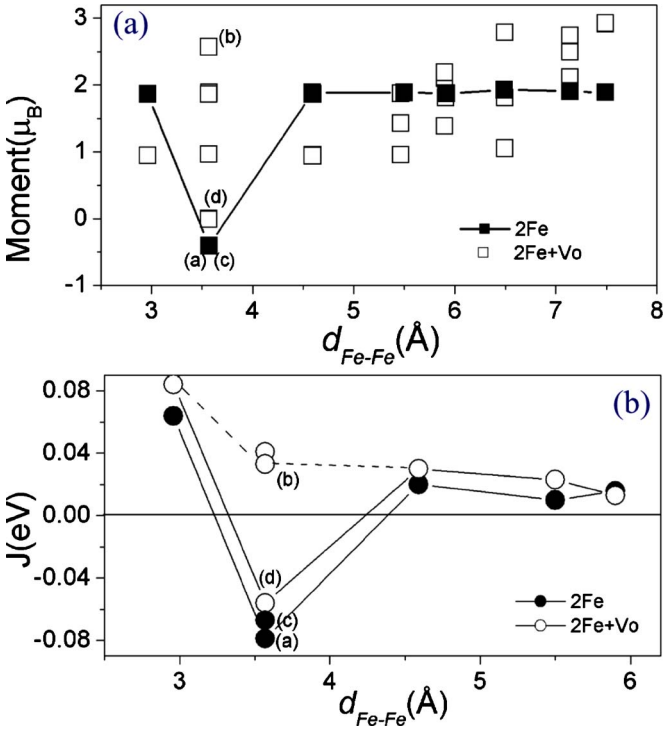

FIG. 4. (Color online) (a) Fe moment in the Fe+V_O model as a function of $d_{Fe\text{-}Fe}$ (open square). The data for 2 Fe with no V_O of Fig. 2 are also shown (solid square). (b) Exchange energy J in the 2 Fe (solid circle) and 2 Fe+V_O (open circle) models. The data points marked (a), (b), (c), (d) correspond to the four cases with $d_{Fe\text{-}Fe}$ =3.57 Å shown in Fig. 5 below.

Fe(d) states ($d^4\uparrow, d^1\downarrow$) and the remaining electron forms a shallow impurity state as illustrated in Figs. 1(c) and 1(d). This electron has Fe-d character (~50%), but also a substantial amount of Ti-d character as well (~40%). This configuration has the lowest energy and the Fe moment is enhanced from 1.67 μ_B when no V_O is present to 1.86 μ_B. Therefore, shallow states would be important in the reduced samples of Fe-doped TiO_2. If the vacancy is further away from the Fe, then both the vacancy electrons occupy the Fe states making it d^6; either $(t_{2g}^3\uparrow, t_{2g}^3\downarrow)$, when Fe is at an intermediate distance from the vacancy or $(d^4\uparrow, d^2\downarrow)$, when Fe is very far from the V_O as shown in Fig. 3. At $d_{Fe\text{-}V}$ slightly above 3.54 Å, both the TE and moments change rapidly. At large $d_{Fe\text{-}V}$, M_S approaches the value of 1.67 μ_B of a single Fe indicating a diminishing influence of V_O. All these show the sensitive dependence of the electronic structure of Fe on the specific location of V_O.

The case of 2 Fe and 1 V_O is the most relevant concentration for real samples. Extensive modeling was carried out to study the influence of V_O on Fe-Fe interactions. The results for the computed moments M_S and the exchange parameter J=E_{AF}-E_F (positive J indicates FM interaction) are shown in Fig. 4. At each $d_{Fe\text{-}Fe}$, several calculations with different V_O locations were carried out. The electronic structure of the Fe atoms depends sensitively on the location of V_O, which in turn results in different values for the magnetic moment. At larger $d_{Fe\text{-}Fe}$, the effect of V_O is to increase the overall Fe moment to about 2.7 μ_B per Fe, a value close to

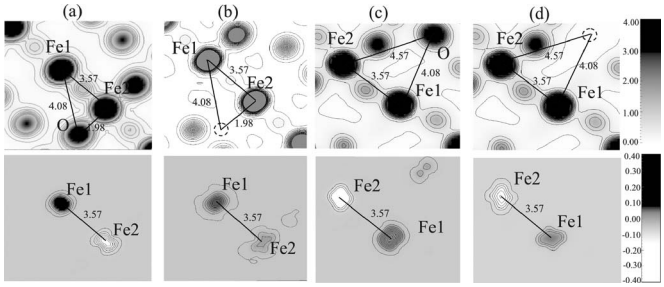

FIG. 5. Charge density (top panel) and spin density (lower panel) (in unit of electron/cell volume) for 2 Fe and 2 Fe+V_O with $d_{Fe\text{-}Fe}$ fixed at 3.57 Å. (a) and (b): reversal of AFM ordering to FM ordering when V_O is at a NN location of Fe2. (c) and (d), the AFM ordering was retained when V_O is farther away from the 2 Fe.

the experimentally reported value[12] of 2.4 μ_B. Of particular interest is the effect of V_O for the special case of $d_{Fe\text{-}Fe}$ =3.57 Å where the 2 Fe moments are AF coupled without V_O. In 5 out of 9 cases, AF coupling persists resulting in almost zero M_S [some configurations have very close M_S values so their data points in Fig. 4(a) cannot be distinguished.] On the other hand, a maximum M_S of 2.57 μ_B occurred at the Fe-V_O separations of 1.98 Å and 4.08 Å with a FM ground state. This is consistent with the result of Fig. 3 that V_O at the NN site enhances the moments. Furthermore, it shows that the AF ordering between two Fe atoms with $d_{Fe\text{-}Fe}$ at 3.57 Å can be reversed to FM ordering by the presence of V_O at the strategic locations. The reversal of this ordering is related to the change in the orbital nature of the Fe state near E_F in the proximity of V_O which now favors the DXC mechanism over the SXC mechanism. When the V_O are further away, its influence on the two Fe atoms ($d_{Fe\text{-}Fe}$ =3.57 Å) is diminished and AF ordering is retained. Again, there are two scenarios here. When V_O is far away from the Fe atoms, Fe becomes more or less d^5, generally with the $(t_{2g}^3\uparrow, t_{2g}^2\downarrow)$ for each Fe atom, so that the magnetic moment is close to 1. An interesting special case is when V_O sits close to one of the Fe atoms, so that a shallow state would have formed in the absence of the other Fe atom. In this case, we find that there is a strong hybridization between the Fe-Fe atoms mediated by the shallow electron. This is kind of a double exchange, where an extra mobile electron mediates a FM interaction. The net interaction is FM.

In Fig. 5, we show the charge density and spin-density of these two cases with $d_{Fe\text{-}Fe}$=3.57 Å without V_O and with V_O in the plane containing Fe-O-Fe or Fe-V_O-Fe. Figures 5(a) and 5(b) shows the reversal of AF to FM when V_O is at the NN site of one of the Fe. Figures 5(c) and 5(d) show that the AF ordering is retained when V_O is further from both Fe. The corresponding DOS and partial DOS of the two Fe atoms are displayed in Fig. 6 for the two cases of Figs. 5(a) and 5(b). The reversal of the directions of moments on the two Fe atoms is clearly shown. The above explanation for the reversal of AF coupling to FM coupling in the presence of V_O is further supported by the calculated exchange energy J between Fe-Fe pairs in these models shown in Fig. 4(b). $|J|$ decreases as $d_{Fe\text{-}Fe}$ increases. In the presence of V_O, J values at $d_{Fe\text{-}Fe}$=3.57 Å can be either positive or negative, or the possibility of the reversal from the AF ordering to the FM ordering.

We have also carried out preliminary investigations for the cases of three Fe substitutions and 1 Fe with 2 V_O. The results are far more complicated, but the main conclusions from the above studies remain valid. For 3 Fe substitutions with no V_O, there is no evidence for Fe atoms to cluster together and the magnetic structure shows evidence of spin frustration at higher Fe concentration.[25] This is in line with recent suggestion that spatial disorder leads to a frustrated spin-glass behavior in MOS.[26] In the case of 1 Fe and 2 V_O, the results suggest that close V_O-V_O distance is energetically unfavorable and the M_s can vary over a wide range from 0.32 μ_B to 2.94 μ_B depending on the locations of the V_O. These and other results will be presented in future publications.

IV. CONCLUSIONS

In conclusion, by considering the concrete example of Fe-doped TiO_2 based on detailed DFT calculations, we showed that V_O plays an important role in the magnetic properties of the dilute oxide magnetic semiconductors. The vacancy enhances the ferromagnetic coupling J between two Fe dopants, either via the formation of a shallow impurity state if the vacancy is close to one of the Fe atoms or by an enhancement of the ferromagnetic double exchange if they are far away. Our results show the rich and complex behavior of reduced Fe-doped TiO_2 that only large scale simulations can reveal. Such information is difficult to obtain purely by experimental means where the sample character cannot be

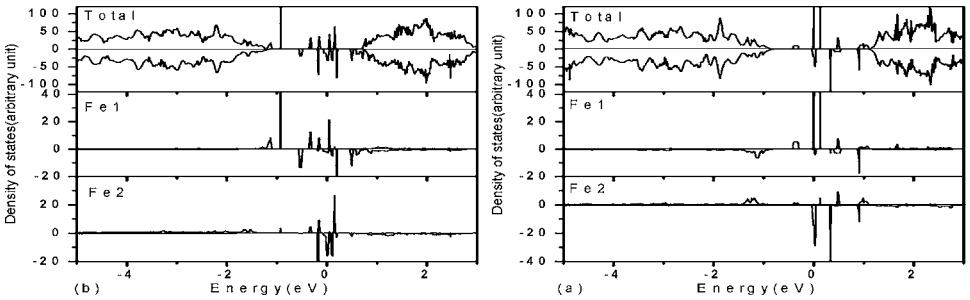

FIG. 6. Left panel: (a) Total DOS, (b) PDOS of Fe1; (c) PDOS for Fe2 in the 2 Fe model without V_O [case of Fig. 5(a)]. Right panel: same as left panel with V_O present [case of Fig. 5(b)]. The positive values are for majority spin channel and the negative values are for the minority spin channel.

strictly controlled. The overall magnetic properties of Fe-doped TiO_2 should be the statistical average of many possible defect configurations corresponding to a real disordered system. It cannot be generalized by a model or models based on perfect ordering of one type or another. For more realistic modeling with more than 2 Fe and 2 V_O, an even larger supercell than used in the present study will be necessary to obtain correct results. Thus the results of many existing calculations on dilute magnetic semiconductors with small supercells cannot be trusted. Obviously, the knowledge and understanding of specific defect types and their preponderance of occurrence will be the key to interpreting the experimental data correctly.

ACKNOWLEDGMENTS

This work is supported by the U.S. DOE under Grant No. DE-FG02-84DR45170. This research used resources of NERSC supported by Office of Science of DOE under Contract No. DE-AC03-76SF00098.

*Corresponding author. Electronic address: chingw@umkc.edu

[1] A. H. Macdonald, P. Schiffer, and N. Samarth, Nat. Mater. **4**, 195–201 (2005).
[2] P. Mahadevan and A. Zunger, Phys. Rev. B **69**, 115211 (2004).
[3] H. Ohno, Science **281**, 951 (1998).
[4] T. Dietl *et al.*, Science **287**, 1019 (2000).
[5] Z. S. Popovic, S. Satpathy, and W. C. Mitchel, Phys. Rev. B **70**, 161308 (2004).
[6] S. A Chambers *et al.*, Appl. Phys. Lett. **79**, 3467 (2001).
[7] Y. Matsumoto *et al.*, Science **291**, 854 (2001).
[8] W. K. Park *et al.*, J. Appl. Phys. **91**, 8093 (2002).
[9] D. H. Kim *et al.*, Appl. Phys. Lett. **81**, 2421 (2002).
[10] J.-Y. Kim *et al.*, Phys. Rev. Lett. **90**, 017401 (2003).
[11] S. A. Chambers *et al.*, Appl. Phys. Lett. **82**, 1257 (2003).
[12] Z. Wang *et al.*, Appl. Phys. Lett. **83**, 518 (2003).
[13] R. Janisch, P. Gopal, and N. A. Spaldin, J. Phys.: Condens. Matter **17**, R657 (2005).
[14] R. Suryanarayanan *et al.*, J. Phys.: Condens. Matter **17**, 755 (2005).
[15] M. S. Park, S. K. Kwon, and B. I. Min, Phys. Rev. B **65**, 161201 (2002).
[16] H. Yang *et al.*, J. Appl. Phys. **93**, 7873 (2003).
[17] E. C. Kim *et al.*, Solid State Commun. **132**, 477 (2004).
[18] L. Errico, M. Weissmann, and M. Renteria, Phys. Status Solidi B **241**, 2399 (2004); Physica B **352**, 338 (2004).
[19] Y. J. Kim *et al.*, Appl. Phys. Lett. **84**, 3531 (2004).
[20] G. Kresse and J. Hafner, Phys. Rev. B **47**, RC558 (1993).
[21] G. Kresse and J. Furthmuller, Comput. Mater. Sci. **6**, 15 (1996); Phys. Rev. B **54**, 11169 (1996).
[22] C. Zener, Phys. Rev. **82**, 403 (1951).
[23] P. W. Anderson and H. Hasegawa, Phys. Rev. **100**, 675 (1955); P.-G. de Gennes, Phys. Rev. **118**, 141 (1960).
[24] H. Meskine, H. Koenig, and S. Satpathy, Phys. Rev. B **64**, 094433 (2001).
[25] G. Zarand and B. Janko, Phys. Rev. Lett. **89**, 047201 (2002).
[26] S-R. Eric Yang and A. H. Macdonald, Phys. Rev. B **67**, 155202 (2003).